IGFBP-4 is an inhibitor of canonical Wnt signaling required for cardiogenesis

Weidong Zhu[1,8], Ichiro Shiojima[1,8], Yuzuru Ito[2,8], Zhi Li[1], Hiroyuki Ikeda[1], Masashi Yoshida[1], Atsuhiko T Naito[1], Jun-ichiro Nishi[1], Hiroo Ueno[3], Akihiro Umezawa[4], Tohru Minamino[1], Toshio Nagai[1], Akira Kikuchi[7], Makoto Asashima[2,5,6], Issei Komuro[1]

[1]Department of Cardiovascular Science and Medicine, Chiba University Graduate School of Medicine, Chiba 260-8670, Japan

[2]ICORP Organ Regeneration Project, Japan Science and Technology Agency (JST), Tokyo 153-8902 Japan.

[3]Department of Pathology and Developmental Biology, Stanford University School of Medicine, Stanford, CA 94305, USA

[4]Department of Reproductive Biology, National Institute for Child Health and Development, Tokyo 157-8535, Japan

[5]Department of Life Sciences (Biology), Graduate School of Arts and Science, The University of Tokyo, Tokyo 153-8902, Japan.

[6]National Institute of Advanced Industrial Sciences and Technology (AIST), Ibaraki 305-8562, Japan.

[7]Department of Biochemistry, Graduate School of Biomedical Sciences, Hiroshima University, Hiroshima 734-8551, Japan.

[8]These authors contributed equally to this work.

Correspondence should be addressed to I.K. (komuro-tky@umin.ac.jp)

Insulin-like growth factor binding proteins (IGFBPs) bind to and modulate the actions of insulin-like growth factors (IGFs)[1]. Although some of the actions of IGFBPs have been reported to be independent of IGFs, the precise mechanisms of IGF-independent actions of IGFBPs are largely unknown[1,2]. Here we report a previously unknown function for IGFBP-4 as a cardiogenic growth factor. IGFBP-4 enhanced cardiomyocyte differentiation *in vitro*, and knockdown of IGFBP-4 attenuated cardiomyogenesis both *in vitro* and *in vivo*. The cardiogenic effect of IGFBP-4 was independent of its IGF binding activity but was mediated by the inhibitory effect on canonical Wnt signaling. IGFBP-4 physically interacted with a Wnt receptor Frizzled 8 (Frz8) and a Wnt co-receptor low-density lipoprotein receptor-related protein 6 (LRP6), and inhibited Wnt3A binding to Frz8 and LRP6. Although IGF-independent, the cardiogenic effect of IGFBP-4 was attenuated by IGFs through IGFBP-4 sequestration. Thus, IGFBP-4 is an inhibitor of canonical Wnt signaling required for cardiogenesis, and provides a molecular link between IGF signaling and Wnt signaling.

The heart is the first organ to form during embryogenesis, and abnormalities in this process result in congenital heart diseases, the most common cause of birth defects in humans[3,4]. Molecules that mediate cardiogenesis are of particular interest because of their potential use for cardiac regeneration[5,6]. Previous studies have shown that soluble growth factors such as bone morphogenetic proteins (BMPs), fibroblast growth factors (FGFs), Wnts, and Wnt inhibitors mediate the tissue interactions critical for cardiomyocyte specification[4,6]. We hypothesized that there might be additional soluble factors that modulate cardiac development and/or cardiomyocyte differentiation.

P19CL6 cells differentiate into cardiomyocytes with high efficiency in the presence of 1% DMSO[7]. We cultured P19CL6 cells with culture media conditioned by various cell types in the absence of DMSO and screened the cardiogenic activity of the conditioned media. The extent of cardiomyocyte differentiation was assessed by the immunostaining with MF20 monoclonal antibody that recognizes sarcomeric myosin heavy chain (MHC). Among the several cell types tested, culture media conditioned by a murine stromal cell line OP9 induced cardiomyocyte differentiation of P19CL6 cells without DMSO treatment (Fig. 1a, left and middle panels). Increased MF20-positive area was accompanied by the induction of cardiac marker genes such as *αMHC*, *Nkx2.5*, and *GATA-4*, and by the increased protein levels of cardiac troponin T (cTnT) (Fig. 1a, right panel). In contrast, culture media conditioned by COS7 cells, mouse embryonic fibroblasts, NIH3T3 cells, HeLa cells, END2 cells (visceral endoderm-like cells), neonatal rat cardiomyocytes, and neonatal rat cardiac fibroblasts did not induce cardiomyocyte differentiation of P19CL6 cells in the absence of DMSO (Fig. 1a and data not shown). From these observations, we postulated that OP9 cells secrete a cardiogenic growth factor(s).

To identify an OP9-derived cardiogenic factor, cDNA clones isolated by a signal sequence trap method from an OP9 cell cDNA library[8] were tested for their cardiogenic activities by transient transfection. When available, recombinant proteins were also used to confirm the results. Among candidate factors tested, IGFBP-4 induced cardiomyocyte differentiation of P19CL6 cells as evidenced by the increase in MF20-positive area and the induction of cardiac markers (Fig. 1b). We also cultured P19CL6 cells with OP9-conditioned media pretreated with an anti-IGFBP-4 neutralizing antibody. The application

of an anti-IGFBP-4 neutralizing antibody attenuated the efficiency of cardiomyocyte differentiation induced by OP9-conditioned media (Fig. 1c). These findings strongly suggest that IGFBP-4 is a cardiogenic factor secreted from OP9 cells.

Since IGFBPs have been characterized as molecules that bind to and modulate the actions of IGFs, we tested whether IGFBP-4 promotes cardiogenesis by either enhancing or inhibiting the actions of IGFs. We first treated P19CL6 cells with a combination of anti-IGF-I and IGF-II neutralizing antibodies or a neutralizing antibody against type-I IGF receptor. If IGFBP-4 induces cardiomyocyte differentiation by inhibiting IGF signaling, treatment with these antibodies should induce cardiomyocyte differentiation and/or enhance the cardiogenic effects of IGFBP-4. On the other hand, if IGFBP-4 promotes cardiogenesis by enhancing IGF signaling, treatment with these antibodies should attenuate IGFBP-4-mediated cardiogenesis. However, treatment with these antibodies did not affect the efficiency of IGFBP-4-induced cardiomyocyte differentiation (Fig. 1d and data not shown). Treatment of P19CL6 cells with IGF-I and –II also did not induce cardiomyocyte differentiation (data not shown). Furthermore, treatment with an IGFBP-4 mutant (IGFBP-4-H74P; His74 replaced by Pro)[9] that is unable to bind IGFs induced cardiomyocyte differentiation of P19CL6 cells even more efficiently than wild type IGFBP-4 (Fig. 1e). This is presumably due to the sequestration of wild type IGFBP-4 but not mutant IGFBP-4-H74P by endogenous IGFs. Consistent with this idea, exogenous IGFs attenuated wild type IGFBP-4- but not IGFBP-4-H74P-induced cardiogenesis (Fig. 1f). Taken together, these observations indicate that IGFBP-4 induces cardiomyocyte differentiation in an IGF-independent fashion.

In order to further explore the mechanisms by which IGFBP-4 induces cardiomyogenesis, we tested the hypothesis that IGFBP-4 might modulate the signals activated by other secreted factors implicated in cardiogenesis. It has been shown that canonical Wnt signaling plays a critical role in cardiomyocyte differentiation[4,6]. In P19CL6 cells, Wnt3A treatment activated β-catenin-dependent transcription of TOPFLASH reporter gene, and this activation was attenuated by IGFBP-4 (Fig. 2a). Wnt/β-catenin signaling is transduced by the cell surface receptor complex consisting of Frizzled and low density lipoprotein receptor (LDLR)-related protein 5/6 (LRP5/6)[10,11], and IGFBP-4 attenuated TOPFLASH activity enhanced by the expression of LRP6 or Frizzled 8 (Frz8) (Fig. 2a). As a control, IGFBP-4 did not alter BMP-mediated activation of a BMP-responsive reporter BRE-luc (Supplementary Fig. S1b). These findings suggest that IGFBP-4 is a specific inhibitor of canonical Wnt pathway. To examine this notion *in vivo*, we performed axis duplication assays in *Xenopus* embryos. Injection of Xwnt8 or LRP6 mRNA caused secondary axis formation, and injection of *Xenopus* IGFBP-4 (XIGFBP-4) mRNA alone had minimal effects on axis formation. However, Xwnt8- or LRP6-induced secondary axis formation was efficiently blocked by co-expression of XIGFBP-4 (Fig. 2b,c), indicating that IGFBP-4 inhibits canonical Wnt signaling *in vivo*. To explore the mechanisms of Wnt inhibition by IGFBP-4, *Xenopus* animal cap assays and TOPFLASH reporter gene assays were performed. In animal cap assays, IGFBP-4 inhibited LRP6-induced but not β-catenin-induced Wnt target gene expression (Supplementary Fig. S1c). Likewise, IGFBP-4 attenuated Wnt3A- or LRP6-induced TOPFLASH activity but did not alter Dishevelled-1 (Dvl-1)-, LiCl-, or β-catenin-induced TOPFLASH activity (Supplementary Fig. S1d,e).

These findings suggest that IGFBP-4 inhibits canonical Wnt signaling at the level of cell surface receptors. To examine whether IGFBP-4 antagonizes Wnt signaling via direct physical interaction with LRP5/6 or Frizzled, we produced conditioned media containing Myc-tagged extracellular portion of LRP6 (LRP6N-Myc), Myc-tagged cysteine-rich domain (CRD) of Frz8 (Frz8CRD-Myc), and V5-tagged IGFBP-4 (IGFBP-4-V5). Immunoprecipitation (IP)/Western experiments revealed that IGFBP-4 interacted with LRP6N (Fig. 2d) and Frz8CRD (Fig. 2e). A liquid-phase binding assay using ^{125}I-labeled IGFBP-4 and conditioned media containing LRP6N-Myc or Frz8CRD-Myc demonstrated that the interaction between IGFBP-4 and LRP6N or Frz8CRD was specific and saturable (Fig. 2f,g). Scatchard plot analysis revealed two binding sites with different binding affinities for LRP6N (Fig. 2f, inset) and a single binding site for Frz8CRD (Fig. 2g, inset). A similar binding assay using ^{125}I-labeled Wnt3A demonstrated that IGFBP-4 inhibited Wnt3A binding to LRP6N (Fig. 2h) and Frz8CRD (Fig. 2i), and Lineweaver-Burk plot revealed that IGFBP-4 was a competitive inhibitor of Wnt3A binding to Frz8CDR (Supplementary Fig. S2a). IP/Western analyses using various deletion mutants of LRP6 and IGFBP-4 revealed that IGFBP-4 interacted with multiple domains of LRP6, and that the carboxy-terminal thyroglobulin domain of IGFBP-4 was required for IGFBP-4 binding to LRP6 or Frz8CRD (Supplementary Fig. S2b-f). It has been shown that inhibition of canonical Wnt signaling promotes cardiomyocyte differentiation in embryonic stem (ES) cells and in chick, *Xenopus*, and zebrafish embryos[12-16]. Thus, these results collectively suggest that IGFBP-4 promotes cardiogenesis by antagonizing Wnt/β-catenin pathway through direct interactions with Frizzled and LRP5/6.

Next we investigated the role of endogenous IGFBP-4 in P19CL6 cell differentiation into cardiomyocytes. RT-PCR analysis revealed that the expression of *IGFBP-4* was upregulated during DMSO-induced P19CL6 cell differentiation (Fig. 3a). Expression of *IGFBP-3* and *–5* was also upregulated in the early and the late phase of differentiation, respectively. Expression of *IGFBP-2* was not altered, and that of *IGFBP-1* or *–6* was not detected. When IGFBP-4 was knocked down by two different small interfering RNA (siRNA) constructs, DMSO-induced cardiomyocyte differentiation was inhibited in both cases (Fig. 3b). In contrast, knockdown of IGFBP-3 or IGFBP-5 did not inhibit DMSO-induced cardiomyocyte differentiation (Fig. 3b, right panel). Treatment with an anti-IGFBP-4 neutralizing antibody also blocked DMSO-induced cardiomyocyte differentiation (Fig. 3c). Thus, secretion of endogenous IGFBP-4 is required for cardiomyocyte differentiation of P19CL6 cells. IGFBP-4 immunostaining revealed that cardiac myocytes were surrounded by the IGFBP-4-positive cells, suggesting that a paracrine effect of IGFBP-4 on cardiomyocyte differentiation is predominant (Fig. 3d). Essentially the same results were obtained in ES cells (Supplementary Fig. S3d-g). To investigate whether IGFBP-4 promotes cardiomyocyte differentiation of P19CL6 cells via inhibition of canonical Wnt pathway, we expressed dominant-negative LRP6 (LRP6N) in P19CL6 cells. Expression of LRP6N enhanced cardiomyocyte differentiation of P19CL6 cells, and reversed the inhibitory effect of IGFBP-4 knockdown on cardiomyogenesis (Fig. 3e). These observations suggest that endogenous IGFBP-4 is required for cardiomyocyte differentiation of P19CL6 cells and ES cells, and that the cardiogenic effect of IGFBP-4 is mediated by its inhibitory effect on Wnt/β-catenin signaling.

The role of endogenous IGFBP-4 in cardiac development *in vivo* was also examined using *Xenopus* embryos. Whole mount *in situ* hybridization analysis revealed that strong expression of *XIGFBP-4* was detected at stage 38 in the anterior part of the liver adjacent to the heart (Fig. 4a). Knockdown of XIGFBP-4 by two different morpholino (MO) constructs resulted in cardiac defects, with more than 70% of the embryos having small or no heart (Fig. 4b). The specificity of MO was confirmed by the observation that co-injection of MO-resistant XIGFBP-4 cDNA rescued the MO-induced cardiac defects (Fig. 4b, Supplementary Fig. S4c). Importantly, co-expression of IGF binding-defective XIGFBP-4 mutant (XIGFBP-4-H74P) or dominant-negative LRP6 (LRP6N) also rescued the cardiac defects induced by XIGFBP-4 knockdown (Fig. 4b), whereas overexpression of Xwnt8 in the heart forming region resulted in cardiac defects similar to those induced by XIGFBP-4 knockdown (Supplementary Fig. S4d-f), supporting the notion that the cardiogenic effect of IGFBP-4 is independent of IGFs but is mediated by inhibition of Wnt/β-catenin pathway. Temporal profile of cardiac defects induced by XIGFBP-4 knockdown was also examined by *cardiac Troponin I* (cTnI) *in situ* hybridization (Fig. 4c). At stage 34, morphology of the heart was comparable between control embryos and MO-injected embryos. However, at stage 38, when *XIGFBP-4* starts to be expressed in the anterior part of the liver, the expression of *cTnI* was markedly attenuated in MO-injected embryos, and expression of *cTnI* was diminished and no heart-like structure was observed at stage 42. Thus, the heart is initially formed but subsequent growth of the heart is perturbed in the absence of XIGFBP-4, suggesting that IGFBP-4 promotes cardiogenesis by maintaining the proliferation and/or survival of embryonic cardiomyocytes.

It has been shown that canonical Wnt signals inhibit cardiogenesis in chick and frog embryos, and that Wnt antagonists such as Dkk1 and Crescent secreted from anterior endoderm or organizer region counteract the Wnt-mediated inhibitory signals and induce cardiogenesis in the anterior lateral mesoderm[13-15]. However, IGFBP-4-mediated Wnt inhibition is required at later stages of development, when the heart is already formed at the ventral portion and starts to grow and remodel to maintain embryonic circulation. It has been shown that Wnt/β-catenin signaling has time-dependent effects on cardiogenesis in ES cells: canonical Wnt signaling in the early phase of ES cell differentiation promotes cardiomyogenesis whereas it inhibits cardiomyocyte differentiation in the late phase[12,16,17]. Consistent with this notion, IGFBP-4 promoted cardiomyocyte differentiation of ES cells only when IGFBP-4 was applied in the late phase after embryoid body formation (Supplementary Fig. S3a-c). Similar time-dependent effects of Wnt/β-catenin signaling on cardiogenesis has been shown in zebrafish embryos[16]. Moreover, several recent reports suggest that Wnt/β-catenin signaling is a positive regulator of cardiac progenitor cell proliferation in the secondary heart field[18-22]. It therefore appears that canonical Wnt signaling has divergent effects on cardiogenesis at multiple stages of development: canonical Wnt signaling (i) promotes cardiogenesis at the time of gastrulation or mesoderm specification, (ii) inhibits cardiogenesis at the time when cardiac mesoderm is specified in the anterior lateral mesoderm, (iii) promotes the expansion of cardiac progenitors in the secondary heart field, and (iv) inhibits cardiogenesis at later stages when the embryonic heart is growing. It is interesting to note that IGFBP-4 is predominantly expressed in the liver. Mouse IGFBP-4 is also strongly expressed in the tissues adjacent to the heart such as

pharyngeal arches and liver bud at E9.5 (Supplementary Fig. S3h). These observations and the results of IGFBP-4 immunostaining in P19CL6 cells and ES cells suggest that IGFBP-4 promotes cardiogenesis in a paracrine fashion. Together with a previous report showing that cardiac mesoderm secretes FGFs and induces liver progenitors in the ventral endoderm[23], these observations suggest that there exist reciprocal paracrine signals between the heart and the liver that coordinately promote the development of each other.

IGFBPs are composed of 6 members, IGFBP-1 to -6. Reporter gene assays and β-catenin stabilization assays revealed that IGFBP-4 was the most potent canonical Wnt inhibitor, and IGFBP-1, -2, and -6 also exhibited modest activities of Wnt inhibition, whereas IGFBP-3 and -5 had no such activity (Supplementary Fig. S5a-c). Consistent with this, IP/Western analyses demonstrated that IGFBP-1, -2, -4, and -6 but not IGFBP-3 or -5 interacted with LRP6 or Frz8CRD (Supplementary Fig. S5d,e). Thus, lack of cardiac phenotypes in IGFBP-4 null mice or IGFBP-3/4/5 triple knockout mice[24] may be due to genetic redundancies between IGFBP-4 and other IGFBPs such as IGFBP-1, -2 and/or -6.

The identification of IGFBP-4 as an inhibitor of Wnt/β-catenin signaling may also have some implications in cancer biology[25]. It was shown that treatment with IGFBP-4 reduces cell proliferation in some cancer cell lines *in vitro*, and that overexpression of IGFBP-4 attenuates the growth of prostate cancer *in vivo*. Decreased serum levels of IGFBP-4 are associated with the risk of breast cancer. Since activation of Wnt signaling is implicated in several forms of malignant tumors[26,27], it is possible that the inhibitory effect of IGFBP-4 on cell proliferation is mediated in part by the inhibition of canonical Wnt signaling.

Methods Summary

Cell Culture

P19CL6 cells and ES cells were cultured and induced to differentiate into cardiomyocytes essentially as described[7,12]. P19CL6 cells (2000 cells/35 mm dish) were treated with various conditioned media for screening of their cardiogenic activities. For siRNA-mediated knockdown, pSIREN-RetroQ vectors (Clontech) ligated with double-strand oligonucleotides were transfected into P19CL6 cells or ES cells, and puromycin-resistant clones were selected.

IP/Western analyses and binding assays

Conditioned media for IP/Western analyses were produced using 293 cells. Binding reactions were performed at 4ºC overnight. ^{125}I-labeling of IGFBP-4 and Wnt3A was performed using IODO-BEADS Iodination Reagent (Pierce). A liquid-phase binding assay was performed essentially as described[28].

Xenopus experiments

Axis duplication assays, animal cap assays, and *in situ* hybridization analyses in *Xenopus* were done essentially as described[29]. Electroporation of mRNA was done at stage 28 essentially as described[30].

Methods

Plasmids and Reagents

cDNA clones for mouse IGFBPs and *Xenopus* IGFBP-4 were purchased from Open Biosystems. XIGFBP-4-H74P mutant was generated by QuickChange Site-Directed Mutagenesis kit (Stratagene). His-tagged human wild type IGFBP-4 and mutant IGFBP-4-H74P (vectors provided by X. Qin)[9] were produced and purified using HisTrap HP Kit (Amersham). Full-length Frz8, Frz8CRD, and LRP6N were provided by X. He[31,32]. Full length LRP6, membrane-bound forms of LRP6 deletion mutants, and Dkk1 were from C. Niehrs[33]. pXwnt8 and pCSKA-Xwnt8 were from J. Christian[34,35]. pCS2-β-catenin was from D. Kimelman[36]. αMHC-GFP was from B. Fleischmann[37]. BRE-luc was from P ten Dijke[38]. pCGN-Dvl-1 was previously described[39]. Soluble forms of LRP6 deletion mutants and probes for *in situ* hybridization analysis (Nkx2.5, cTnI, and Hex) were generated by PCR. IGFBP-4, Wnt3A, IGF-I, IGF-II, and BMP2 were from R&D. Neutralizing antibodies were from R&D (anti-IGFBP-4), Sigma (anti-IGF-I and anti-IGF-II), and Oncogene (anti-type-I IGF receptor). The antibodies used for IP, Western blotting, and immunostaining were from Invitrogen (anti-Myc, anti-V5), Santa Cruz (anti-cTnT, anti-IGFBP-4, anti-topoisomerase I (TOPO-I)), Sigma (anti-β-actin, anti-β-catenin, anti-FLAG (M2)), and Developmental Studies Hybridoma Bank (anti-sarcomeric myosin heavy chain (MF20)).

Cell Culture Experiments

P19CL6 cells and ES cells were cultured and induced to differentiate into cardiomyocytes essentially as described[7,12]. P19CL6 cells (2000 cells/35 mm dish) were treated with various conditioned media for screening of their cardiogenic activities. P19CL6 cells or ES cells

stably transfected with αMHC promoter driven-green fluorescence protein (GFP) were generated by transfection of αMHC-GFP plasmid into P19CL6 cells or ht7 ES cells followed by G418 selection. Luciferase reporter gene assays, Western blot analyses, immunostaining, and RT-PCR were performed as described[12]. Reporter gene assays were repeated at least three times. PCR primers and PCR conditions are listed in Supplementary Table S1. For siRNA-mediated knockdown, siRNAs were expressed using pSIREN-RetroQ vector (Clontech). Oligonucleotide sequences used are listed in Supplementary Table S2. pSIREN-RetroQ vectors ligated with double-strand oligonucleotides were transfected into P19CL6 cells or ES cells, and puromycin-resistant clones were isolated and expanded. For β-catenin stabilization assays, nuclear extracts of L cells were prepared using NE-PER Nuclear and Cytoplasmic Extraction Reagents (Pierce). Data are shown as mean ± standard deviation.

IP/Western analyses and binding assays

Conditioned media for IP/Western analyses containing full length or various deletion mutants of IGFBPs, LRP6, Frz8CRD, and Dkk1 were produced using 293 cells. Binding reactions were performed at 4ºC overnight. IP was performed using Protein G Sepharose 4 Fast Flow (Amersham). ^{125}I-labeling of IGFBP-4 and Wnt3A was performed using IODO-BEADS Iodination Reagent (Pierce). A liquid-phase binding assay was performed essentially as described[28]. In brief, conditioned media containing LRP6N-Myc or Frz8CRD-Myc were mixed with various concentrations of ^{125}I-labeled IGFBP-4, and incubated at 4ºC overnight. LRP6N-Myc or Frz8CRD-Myc was immunoprecipitated, and radioactivity of bound IGFBP-4 was measured after extensive washing of the Protein G

sepharose beads. For a competitive binding assay, conditioned media containing LRP6N-Myc or Frz8CRD-Myc were mixed with ^{125}I-labeled Wnt3A and cold IGFBP-4, and incubated at 4ºC overnight. LRP6N-Myc or Frz8CRD-Myc was then immunoprecipitated, and radioactivity of bound Wnt3A was measured.

***Xenopus* experiments and mouse *in situ* hybridization analysis**

Axis duplication assays, animal cap assays, and *in situ* hybridization analyses in *Xenopus* were done essentially as described[29]. Two independent cDNAs for XIGFBP-4, presumably resulting from pseudotetraploid genomes, were identified by 5' RACE (Supplementary Fig. S4a). Two different MOs that target both of these two IGFBP-4 transcripts were designed (Gene Tools) (Supplementary Fig. S4a and Supplementary Table S2). MO-sensitive XIGFBP-4 cDNA that includes 41bp 5'-UTR was generated by PCR. MO-resistant XIGFBP-4 cDNA (wild type and H74P mutant) was generated by introducing five silent mutations in the MO1 target sequence and excluding the 5'-UTR (Supplementary Fig. S4a). To determine the specificity of MOs, MO-sensitive or MO-resistant *XIGFBP-4-Myc* mRNA was injected into *Xenopus* embryos with or without MOs, and protein/mRNA expression was analyzed. PCR primers and PCR conditions are listed in Supplementary Table S1. MOs and plasmid DNAs were injected at the 8-cell stage into the dorsal region of two dorsal-vegetal blastomeres fated to be heart and liver anlage. Electroporation of mRNA was done essentially as described[30]. Injection of mRNA (5 ng in 5 nl solution) into the vicinity of heart anlage and application of electric pulses was performed at stage 28. Whole mount *in situ* hybridization analysis of murine IGFBP-4 was performed as described[40].

References

1. Firth, S. M. & Baxter, R. C. Cellular actions of the insulin-like growth factor binding proteins. *Endocr Rev* **23**, 824-54 (2002).
2. Mohan, S. & Baylink, D. J. IGF-binding proteins are multifunctional and act via IGF-dependent and -independent mechanisms. *J Endocrinol* **175**, 19-31 (2002).
3. Srivastava, D. Genetic assembly of the heart: implications for congenital heart disease. *Annu Rev Physiol* **63**, 451-69 (2001).
4. Olson, E. N. & Schneider, M. D. Sizing up the heart: development redux in disease. *Genes Dev* **17**, 1937-56 (2003).
5. Leri, A., Kajstura, J. & Anversa, P. Cardiac stem cells and mechanisms of myocardial regeneration. *Physiol Rev* **85**, 1373-416 (2005).
6. Foley, A. & Mercola, M. Heart induction: embryology to cardiomyocyte regeneration. *Trends Cardiovasc Med* **14**, 121-5 (2004).
7. Monzen, K. *et al*. Bone morphogenetic proteins induce cardiomyocyte differentiation through the mitogen-activated protein kinase kinase kinase TAK1 and cardiac transcription factors Csx/Nkx-2.5 and GATA-4. *Mol Cell Biol* **19**, 7096-105 (1999).
8. Ueno, H. *et al*. A stromal cell-derived membrane protein that supports hematopoietic stem cells. *Nat Immunol* **4**, 457-63 (2003).
9. Qin, X., Strong, D. D., Baylink, D. J. & Mohan, S. Structure-function analysis of the human insulin-like growth factor binding protein-4. *J Biol Chem* **273**, 23509-16 (1998).

10. Moon, R. T., Kohn, A. D., De Ferrari, G. V. & Kaykas, A. WNT and beta-catenin signalling: diseases and therapies. *Nat Rev Genet* **5**, 691-701 (2004).

11. Kikuchi, A., Yamamoto, H. & Kishida, S. Multiplicity of the interactions of Wnt proteins and their receptors. *Cell Signal* **19**, 659-71 (2007).

12. Naito, A. T. *et al*. Developmental stage-specific biphasic roles of Wnt/beta-catenin signaling in cardiomyogenesis and hematopoiesis. *Proc Natl Acad Sci U S A* **103**, 19812-7 (2006).

13. Tzahor, E. & Lassar, A. B. Wnt signals from the neural tube block ectopic cardiogenesis. *Genes Dev* **15**, 255-60 (2001).

14. Schneider, V. A. & Mercola, M. Wnt antagonism initiates cardiogenesis in Xenopus laevis. *Genes Dev* **15**, 304-15 (2001).

15. Marvin, M. J., Di Rocco, G., Gardiner, A., Bush, S. M. & Lassar, A. B. Inhibition of Wnt activity induces heart formation from posterior mesoderm. *Genes Dev* **15**, 316-27 (2001).

16. Ueno, S. *et al*. Biphasic role for Wnt/beta-catenin signaling in cardiac specification in zebrafish and embryonic stem cells. *Proc Natl Acad Sci U S A* **104**, 9685-90 (2007).

17. Liu, Y. *et al*. Sox17 is essential for the specification of cardiac mesoderm in embryonic stem cells. *Proc Natl Acad Sci U S A* **104**, 3859-64 (2007).

18. Lin, L. *et al*. Beta-catenin directly regulates Islet1 expression in cardiovascular progenitors and is required for multiple aspects of cardiogenesis. *Proc Natl Acad Sci U S A* **104**, 9313-8 (2007).

19. Ai, D. *et al*. Canonical Wnt signaling functions in second heart field to promote right ventricular growth. *Proc Natl Acad Sci U S A* **104**, 9319-24 (2007).

20. Kwon, C. *et al*. Canonical Wnt signaling is a positive regulator of mammalian cardiac progenitors. *Proc Natl Acad Sci U S A* **104**, 10894-9 (2007).

21. Cohen, E. D. *et al*. Wnt/beta-catenin signaling promotes expansion of Isl-1-positive cardiac progenitor cells through regulation of FGF signaling. *J Clin Invest* **117**, 1794-804 (2007).

22. Qyang, Y. *et al*. The Renewal and Differentiation of Isl1+ Cardiovascular Progenitors Are Controlled by a Wnt/beta-Catenin Pathway. *Cell Stem Cell* **1**, 165-79 (2007).

23. Jung, J., Zheng, M., Goldfarb, M. & Zaret, K. S. Initiation of mammalian liver development from endoderm by fibroblast growth factors. *Science* **284**, 1998-2003 (1999).

24. Ning, Y. *et al*. Diminished growth and enhanced glucose metabolism in triple knockout mice containing mutations of insulin-like growth factor binding protein-3, -4, and -5. *Mol Endocrinol* **20**, 2173-86 (2006).

25. Durai, R. *et al*. Biology of insulin-like growth factor binding protein-4 and its role in cancer (review). *Int J Oncol* **28**, 1317-25 (2006).

26. Logan, C. Y. & Nusse, R. The Wnt signaling pathway in development and disease. *Annu Rev Cell Dev Biol* **20**, 781-810 (2004).

27. Clevers, H. Wnt/beta-catenin signaling in development and disease. *Cell* **127**, 469-80 (2006).

28. Semenov, M. V. *et al.* Head inducer Dickkopf-1 is a ligand for Wnt coreceptor LRP6. *Curr Biol* **11**, 951-61 (2001).

29. Kobayashi, H. *et al.* Novel Daple-like protein positively regulates both the Wnt/beta-catenin pathway and the Wnt/JNK pathway in Xenopus. *Mech Dev* **122**, 1138-53 (2005).

30. Sasagawa, S., Takabatake, T., Takabatake, Y., Muramatsu, T. & Takeshima, K. Improved mRNA electroporation method for Xenopus neurula embryos. *Genesis* **33**, 81-5 (2002).

31. He, X. *et al.* A member of the Frizzled protein family mediating axis induction by Wnt-5A. *Science* **275**, 1652-4 (1997).

32. Tamai, K. *et al.* LDL-receptor-related proteins in Wnt signal transduction. *Nature* **407**, 530-5 (2000).

33. Mao, B. *et al.* LDL-receptor-related protein 6 is a receptor for Dickkopf proteins. *Nature* **411**, 321-5 (2001).

34. Christian, J. L., McMahon, J. A., McMahon, A. P. & Moon, R. T. Xwnt-8, a Xenopus Wnt-1/int-1-related gene responsive to mesoderm-inducing growth factors, may play a role in ventral mesodermal patterning during embryogenesis. *Development* **111**, 1045-55 (1991).

35. Christian, J. L. & Moon, R. T. Interactions between Xwnt-8 and Spemann organizer signaling pathways generate dorsoventral pattern in the embryonic mesoderm of Xenopus. *Genes Dev* **7**, 13-28 (1993).

36. Yost, C. *et al.* The axis-inducing activity, stability, and subcellular distribution of beta-catenin is regulated in Xenopus embryos by glycogen synthase kinase 3. *Genes Dev* **10**, 1443-54 (1996).

37. Kolossov, E. *et al.* Identification and characterization of embryonic stem cell-derived pacemaker and atrial cardiomyocytes. *FASEB J* **19**, 577-9 (2005).

38. Korchynskyi, O. & ten Dijke, P. Identification and functional characterization of distinct critically important bone morphogenetic protein-specific response elements in the Id1 promoter. *J Biol Chem* **277**, 4883-91 (2002).

39. Kishida, M. *et al.* Synergistic activation of the Wnt signaling pathway by Dvl and casein kinase Iepsilon. *J Biol Chem* **276**, 33147-55 (2001).

40. Hosoda, T. *et al.* A novel myocyte-specific gene Midori promotes the differentiation of P19CL6 cells into cardiomyocytes. *J Biol Chem* **276**, 35978-89 (2001).

Acknowledgement

We thank E. Fujita, R. Kobayashi, and Y. Ishiyama for technical support, X Qin, X He, C Niehrs, J. Christian, D. Kimelman, B. Fleischmann, and P ten Dijke for reagents, T. Yamauchi and K. Ueki for advice on binding assays, Y. Onuma and S. Takahashi for advice on *Xenopus* electroporation. This work was supported by grants from the Ministry of Education, Culture, Sports, Science and Technology (MEXT), the Ministry of Health, Labour, and Welfare, and New Energy and Industrial Technology Development Organization (NEDO).

Author Contribution

W.Z., I.S., and Y.I. contributed equally to this work. I.K. designed and supervised the research, W.Z., I.S., Y.I., Z.L., H.I., M.Y., and A.T.N. performed experiments, J.N., H.U., A.U., T.M., T.N., A.K., and M.A. contributed new reagents/analytical tools, W.Z., I.S., Y.I., A.K., and I.K. analyzed data, and W.Z., I.S., Y.I., and I.K. prepared the manuscript.

Competing Interests Statement

The authors declare no competing financial interests.

Figure Legends

Figure 1. IGFBP-4 promotes cardiomyocyte differentiation in an IGF-independent manner.

a, Culture media conditioned by OP9 cells but not COS7 cells induced cardiomyocyte differentiation of P19CL6 cells as assessed by MF20-positive area, cardiac marker gene expression, and cTnT protein expression. Scale bar=100 μm. **b,** Treatment with IGFBP-4 (1 μg/ml) induced cardiomyocyte differentiation of P19CL6 cells in the absence of DMSO. **c,** Treatment with a neutralizing antibody against IGFBP-4 (αBP4, 40 μg/ml) attenuated cardiomyocyte differentiation of P19CL6 cells induced by OP9-conditioned media. **d,** Treatment with neutralizing antibodies against IGF-I and IGF-II (αIGFs, 5 μg/ml each) had no effect on IGFBP-4-induced cardiomyocyte differentiation of P19CL6 cells. **e,** Mutant IGFBP-4 (IGFBP-4-H74P) that is incapable of binding to IGFs retained cardiomyogenic activity. **f,** IGFs (100 ng/ml each) attenuated wild type IGFBP-4-induced but not mutant IGFBP-4-H74P-induced cardiomyocyte differentiation of P19CL6 cells.

Figure 2. IGFBP-4 inhibits Wnt/β-catenin signaling through direct interactions with Wnt receptors.

a, IGFBP-4 attenuated β-catenin-dependent transcription in P19CL6 cells. P19CL6 cells were transfected with TOPFLASH reporter gene and expression vectors for LRP6 or Frz8, treated with Wnt3A or Wnt3A plus IGFBP-4, and luciferase activities were measured. **b,** XIGFBP-4 inhibited Xwnt8-induced secondary axis formation in *Xenopus* embryos (N=20 for each group). **c,** IGFBP-4 inhibited LRP6-induced secondary axis formation in *Xenopus* embryos (N=30 for each group). **d,e,** IGFBP-4 directly interacted with LRP6N (**d**) and

Frz8CRD (**e**). **f,** A binding assay between ^{125}I-labeled IGFBP-4 and LRP6N. Inset is a scatchard plot showing two binding sites with different binding affinities. **g,** A binding assay between ^{125}I-labeled IGFBP-4 and Frz8CRD. Inset is a scatchard plot showing a single binding site. **h,i,** IGFBP-4 inhibited Wnt3A binding to LRP6N (**h**) or Frz8CRD (**i**). ^{125}I-labeled Wnt3A binding to LRP6N or Frz8CRD was assessed in the presence of increasing amounts of IGFBP-4.

Figure 3. IGFBP-4 is required for cardiomyocyte differentiation of P19CL6 cells.

a, Expression analysis of IGFBP family members by RT-PCR during DMSO-induced cardiomyocyte differentiation of P19CL6 cells (from day 0 to day 8). **b,** Knockdown of IGFBP-4 in P19CL6 cells attenuated cardiac marker expression in response to DMSO treatment (left). BP4-1 and BP4-2 represent two different siRNAs for IGFBP-4. Knockdown of IGFBP-3 or IGFBP-5 had no effect on cTnT expression in response to DMSO treatment (right). **c,** Treatment with a neutralizing antibody against IGFBP-4 (αBP4, 40 μg/ml) attenuated DMSO-induced cardiomyocyte differentiation of P19CL6 cells. **d,** IGFBP-4 immunostaining during DMSO-induced differentiation of P19CL6 cells stably transfected with αMHC-GFP reporter gene. Upper left, IGFBP-4 staining (red); upper right, GFP expression representing differentiated cardiomyocytes; lower left, nuclear staining by DAPI; lower right, a merged picture. Scale bar=100 μm. **e,** Attenuated cardiomyocyte differentiation of P19CL6 cells by IGFBP-4 knockdown was rescued by inhibiting Wnt/β-catenin signaling. Control and IGFBP-4-knocked-down P19CL6 cells were transfected with an expression vector for GFP or LRP6N (a dominant-negative form of LRP6), and induced to differentiate into cardiomyocytes by DMSO treatment. LRP6N overexpression rescued

the attenuated cardiomyocyte differentiation induced by IGFBP-4 knockdown as assessed by MF20-positive area (left panel), cardiac marker gene expression, and cTnT protein expression (right panel).

Figure 4. IGFBP-4 is required for the maturation of the heart in *Xenopus* embryos.

a, *In situ* hybridization analysis of *Nkx2.5* (an early cardiac marker), *cTnI* (a mature cardiac marker), *Hex* (a liver marker), and *XIGFBP-4* mRNA expression at stage 34, 38, and 42. **b,** Knockdown of XIGFBP-4 by two different morpholinos (MO1 and MO2) resulted in severe cardiac defects as assessed by *cTnI in situ* hybridization at stage 42 (left). These cardiac defects were rescued by co-injection of MO-resistant wild type XIGFBP-4, mutant XIGFBP-4-H74P, and LRP6N (N=30 for each group). **c,** Temporal profile of cardiac defects induced by XIGFBP-4 knockdown. Morphology of the heart as assessed by cTnI *in situ* hybridization was almost normal at stage 34 but was severely perturbed at stage 38 and 42. Right column shows sections of control and MO-injected embryos. Arrow indicates the heart in control embryos. No heart-like structure was observed in MO-injected embryos.

Supplementary Figure Legends

Supplementary Figure S1. Inhibition of canonical Wnt pathway by IGFBP-4.

a, IGFBP-4 did not alter FOPFLASH activity. FOPFLASH activity was measured in P19CL6 cells as a control experiment shown in Fig. 2a. **b,** IGFBP-4 did not alter BMP-induced activation of BRE-luc reporter gene. BMP-responsive BRE-luc was activated by BMP2 in a dose-dependent manner (left), and this activation was not altered by IGFBP-4 (right). **c,** Animal cap assays. RNA was injected into the animal pole of two-cell embryos, and the animal caps were dissected at stage 8.5. Expression of Wnt target genes (Siamois and Xnr-3) induced by LRP6 but not by β-catenin was attenuated by XIGFBP-4. **d,e,** TOPFLASH reporter gene assays. IGFBP-4 inhibited canonical Wnt signaling activated by Wnt3A (**d,** left) or LRP6 (**d,** right). However, IGFBP-4 did not inhibit canonical Wnt pathway activated by β-catenin, Dishevelled-1 (Dvl-1) (**e,** left), or GSK3 inhibitor LiCl (**e,** right). TOPFLASH reporter gene assays shown in **b,d,e** were performed in 293 cells.

Supplementary Figure S2. Interaction of IGFBP-4 with Frz8/LRP6.

a, A binding assay between ^{125}I-labeled Wnt3A and Frz8CRD in the absence or the presence of different doses of IGFBP-4 (rectangles, no IGFBP-4; circles, IGFBP-4 (50nM); triangles, IGFBP-4 (100nM)). Inset is a Lineweaver-Burk plot showing that IGFBP-4 is a competitive inhibitor of Wnt3A binding to Frz8CRD. **b,** Schematic illustration of LRP6 deletion mutants used in this study. All deletion mutants are soluble forms. SP, signal peptide; β-pro, β-propeller domain; EGF, EGF-like domain; LDLR, LDL receptor typeA repeats; TM, transmembrane domain. **c-e,** IGFBP-4 interacts with multiple domains of LRP6. As assessed by IP/Western analyses, IGFBP-4 interacted with LRP6N and E1-4

mutants of LRP6 (**c**), E1-2/L, E3-4/L, and L mutants of LRP6 (**d**), and E1-2, E3-4, and L mutants of LRP6 (**e**). As a control, Dkk1 interacted predominantly with E3-4 mutant of LRP6 (**e**). NS represents non-specific bands. **f,** Carboxy-terminal thyroglobulin domain of IGFBP-4 is required for interaction with Frz8/LRP6. Deletion mutants of IGFBP-4 used are shown on the left panel. IGF and TG represent an IGF-binding domain and a thyroglobulin domain, respectively. Full length (FL) and ΔN mutant of IGFBP-4 interacted with Frz8/LRP6 but ΔC mutant did not.

Supplementary Figure S3. IGFBP-4 promotes cardiomyocyte differentiation of ES cells in a paracrine fashion.

a-c, ES cells stably transfected with αMHC-GFP reporter gene were induced to differentiate into cardiomyocytes by a hanging drop method. IGFBP-4 (1 μg/ml) suppressed cardiomyocyte differentiation of ES cells when applied from day 0 to day 3 (D0-3), whereas it enhanced cardiogenesis when applied from day 3 to day 5 (D3-5). The extent of cardiomyocyte differentiation was assessed by GFP-positive area (**a,b**), cardiac marker gene expression (**c,** upper panel), and cTnT protein expression (**c,** lower panel). Scale bar=200 μm. **d,** Expression analysis of IGFBP family members by RT-PCR during cardiomyocyte differentiation of ES cells. **e,** Knockdown of IGFBP-4 in ES cells attenuated cardiac marker gene expression (left) and cardiomyocyte differentiation as assessed by GFP-positive area and cTnT expression (right). BP4-1 and BP4-2 represent two different siRNAs for IGFBP-4. Knockdown of IGFBP-3 or IGFBP-5 had no effect on cardiomyocyte differentiation (right). **f,** Treatment with a neutralizing antibody against IGFBP-4 (αBP4, 40 μg/ml) attenuated cardiomyocyte differentiation of ES cells as assessed by GFP-positive

area, cardiac marker gene expression, and cTnT protein expression. **g,** IGFBP-4 immunostaining during cardiomyocyte differentiation of ES cells stably transfected with αMHC-GFP reporter gene. Upper left, IGFBP-4 staining (red); upper right, GFP expression representing differentiated cardiomyocytes; lower left, nuclear staining by DAPI; lower right, a merged picture. Scale bar=100 μm. h, *In situ* hybridization analysis of murine IGFBP-4 at E9.5. Strong signals were detected in pharyngeal arches, liver bud, and limb buds. S, sense probe; AS, antisense probe.

Supplementary Figure S4. Knockdown of XIGFBP-4 or activation of Wnt pathway disrupts normal cardiac development in *Xenopus* embyros.

a, Sequences of two XIGFBP-4 alleles and positions of MO target sequences are indicated. MO-sensitive and MO-resistant XIGFBP-4 cDNA sequences are also shown. Initiation codon is indicated by red, and mismatches introduced to generate MO-resistant XIGFBP-4 cDNA are shown by underlines. MO-s and MO-r represent MO-sensitive and MO-resistant XIGFBP-4 cDNA, respectively. **b,** Verification of MO activity and specificity. MO-sensitive and MO-resistant *XIGFBP-4-Myc* mRNA was injected into *Xenopus* embryos. Expressions of XIGFBP-4-Myc protein translated from MO-sensitive mRNA were downregulated by co-injection of MO1 or MO2, whereas those of XIGFBP-4-Myc protein translated from MO-resistant mRNA were not. RT-PCR analysis showed comparable amounts of injected mRNA. ODC represents ornithine decarboxylase and served as RT-PCR controls. **c,** Specificities of cardiac phenotypes induced by XIGFBP-4 MOs. Cardiac defects induced by XIGFBP-4 MO1 or MO2 were rescued by co-injection of MO-resistant XIGFBP-4 cDNA (N=30 for each group). **d,** Activation of Wnt pathway disrupts normal

heart development. For Wnt activation in the heart forming region, plasmid DNA encoding Xwnt8 under the control of cytoskeletal actin promoter (pCSKA-Xwnt8) was injected at the 8-cell stage into the dorsal region of two dorsal-vegetal blastomeres fated to be heart and liver anlage. When compared to control embryos (upper panel), Wnt activation by pCSKA-Xwnt8 injection resulted in the attenuation of heart size at stage 42 (lower panel). **e,** Activation of Wnt pathway in the late phase of embryogenesis is sufficient to perturb cardiogenesis. Xwnt8 mRNA was introduced into the vicinity of heart anlage by electroporation at stage 28. GFP mRNA was co-injected to evaluate the efficiency of electroporation. At stage 34, GFP expression was observed at the heart forming area (upper panel, anterior to the left and dorsal is up). When compared to control embryos injected with GFP mRNA alone (middle panel), embryos injected with Xwnt8 and GFP mRNA exhibited abnormal heart morphogenesis at stage 42 (lower panel). **f,** A quantitative analysis of the effects of Wnt activation on cardiac development.

Supplementary Figure S5. Wnt inhibition by IGFBPs.

a, β-catenin stabilization assays in L cells. Treatment with Wnt3A induced a robust increase in the amount of nuclear β-catenin, which was reversed by IGFBP-4. **b,c,** β-catenin stabilization assays (**b**) and TOPFLASH reporter gene assays (**c**) in the absence or the presence of IGFBPs. IGFBPs were added at the concentration of 500ng/ml. **d,e,** IP/Western analyses to examine the physical interactions between IGFBPs and LRP6 (**d**) or Frz8CRD (**e**). IGFBP-1, -2, -4, and -6 interacted with LRP6/Frz8CRD, whereas IGFBP-3 and -5 did not.

Supplementary Table S1. PCR primers and PCR conditions

Gene	Primers	PCR product (bp)	Annealing (C°)
αMHC	5'-GGAAGAGTGAGCGGCCATCAAGG-3' 5'-CTGCTGGAGAGGTTATTCCTCG-3'	302	65
Nkx2.5	5'-CAGTGGAGCTGGACAAAGCC-3' 5'-TAGCGACGGTTCTGGAATTT-3'	216	55
GATA-4	5'-CTGTCATCTCACTATGGGCA-3' 5'-CCAAGTCCGAGCAGGAATTT-3'	275	60
β-actin	5'-GGACCTGGCTGGCCGGGACC-3' 5'-GCGGTGCACGATGGAGGGGC-3'	583	60
IGFBP-1	5'-CCAGGGATCCAGCTGCCGTGCG-3' 5'-GGCGTTCCACAGGATGGGCTG-3'	259	60
IGFBP-2	5'-CAACTGTGACAAGCATGGCCG-3' 5'-CACCAGTCTCCTGCTGCTCGT-3'	176	60
IGFBP-3	5'-GACACCCAGAACTTCTCCTCC-3' 5'-CATACTTGTCCACACACCAGC-3'	220	60
IGFBP-4	5'-CGTCCTGTGCCCCAGGGTTCCT-3' 5'-GAAGCTTCACCCCTGTCTTCCG-3'	200	60
IGFBP-5	5'-GTTTGCCTCAACGAAAAGAGCT-3' 5'-CTGCTTTCTCTTGTAGAATCCTT-3'	393	60
IGFBP-6	5'-CCCCGAGAGAACGAAGAGACG-3' 5'-CTGCGAGGAACGACACTGCTG-3'	351	60
XIGFBP-4 (MO-s)	5'-CAAACTCATTCATCTCCAGCCC-3' 5'-TTCCTTTCCCCTCTCAGATGCC-3'	808	55
XIGFBP-4 (MO-r)	5'-ATGTCAGGTTACTGTCATCCTGCCC-3' 5'-TTCCTTTCCCCTCTCAGATGCC-3'	767	55
Siamois	5′-TACCGCACTGACTCTGCAAG-3′ 5′-CTGAGGCTCCTGTGGAATTC-3′	192	62
Xnr-3	5′-CTTCTGCACTAGATTCTG-3′ 5′-CAGCTTCTGGCCAAGACT-3′	281	58
ODC	5'-GTCAATGATGGAGTGTATGGATC-3' 5'-TCCAATCCGCTCTCCTGAGCAC-3'	386	55

Supplementary Table S2. Oligonucleotide sequences for siRNAs and morpholinos

Gene	Oligonucleotide Sequences
mIGFBP-3	AATCCTAGATGAAGTGTTA
mIGFBP-4-1	GAGCCAGGCTGCGGTTGTT
mIGFBP-4-2	GCAAGTGCTGGTGTGTGGA
mIGFBP-5	AAGGCCTCCAAGCTAATTA
XIGFBP-4-MO1	GCAGGGTGGCAATATCCAGACATGA
XIGFBP-4-MO2	CTTGCTGGGCTGGAGATGAATGAGT

Figure 1

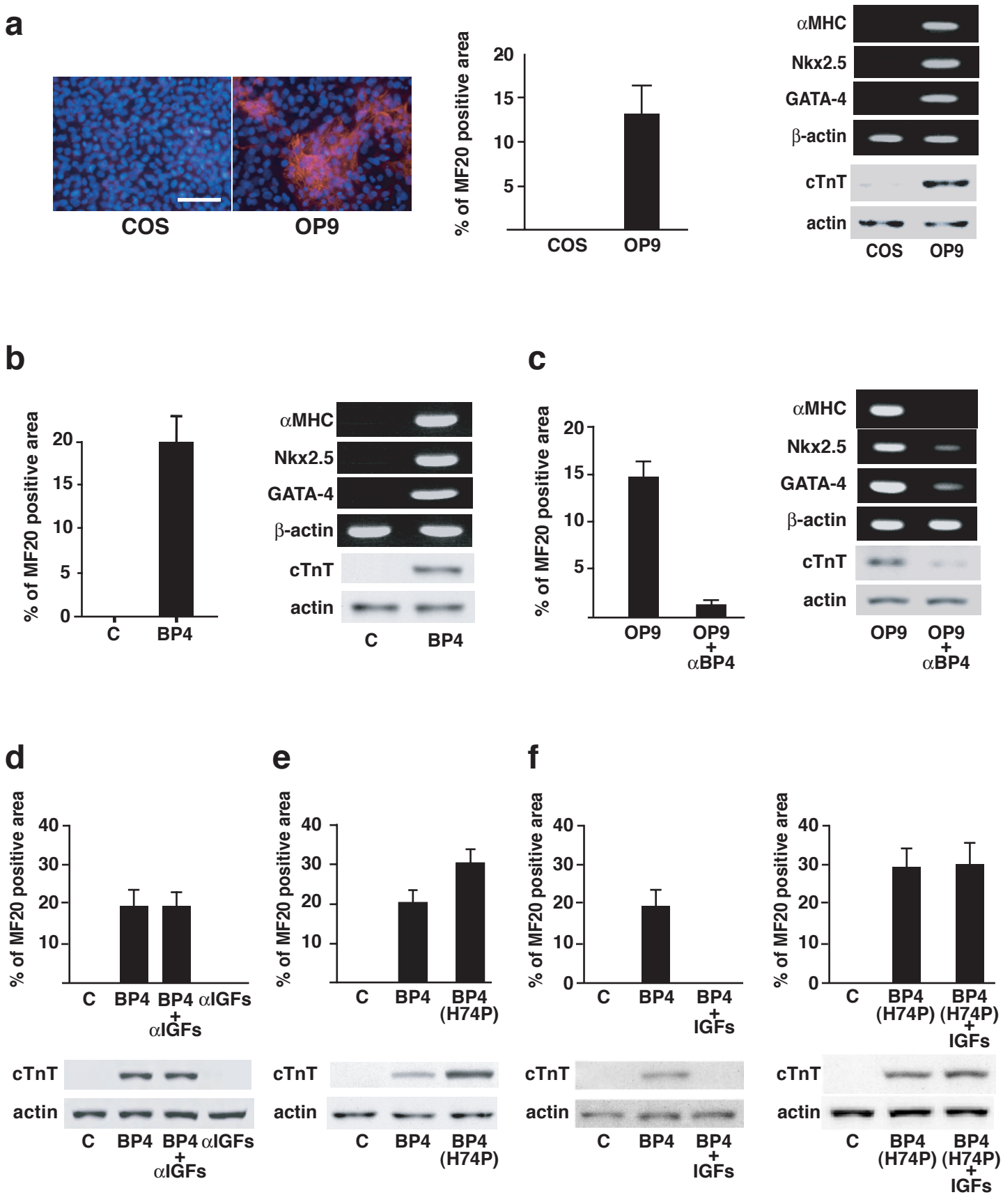
a
COS
OP9
% of MF20 positive area
20
15
10
5
COS
OP9
αMHC
Nkx2.5
GATA-4
β-actin
cTnT
actin
COS
OP9
b
% of MF20 positive area
20
15
10
5
0
C
BP4
αMHC
Nkx2.5
GATA-4
β-actin
cTnT
actin
C
BP4
c
% of MF20 positive area
20
15
10
5
OP9
OP9 + αBP4
αMHC
Nkx2.5
GATA-4
β-actin
cTnT
actin
OP9
OP9 + αBP4
d
% of MF20 positive area
40
30
20
10
C
BP4
BP4 + αIGFs
αIGFs
cTnT
actin
C
BP4
BP4 + αIGFs
αIGFs
e
% of MF20 positive area
40
30
20
10
C
BP4
BP4 (H74P)
cTnT
actin
C
BP4
BP4 (H74P)
f
% of MF20 positive area
40
30
20
10
0
C
BP4
BP4 + IGFs
% of MF20 positive area
40
30
20
10
0
C
BP4 (H74P)
BP4 (H74P) + IGFs
cTnT
actin
C
BP4
BP4 + IGFs
cTnT
actin
C
BP4 (H74P)
BP4 (H74P) + IGFs

Figure 2

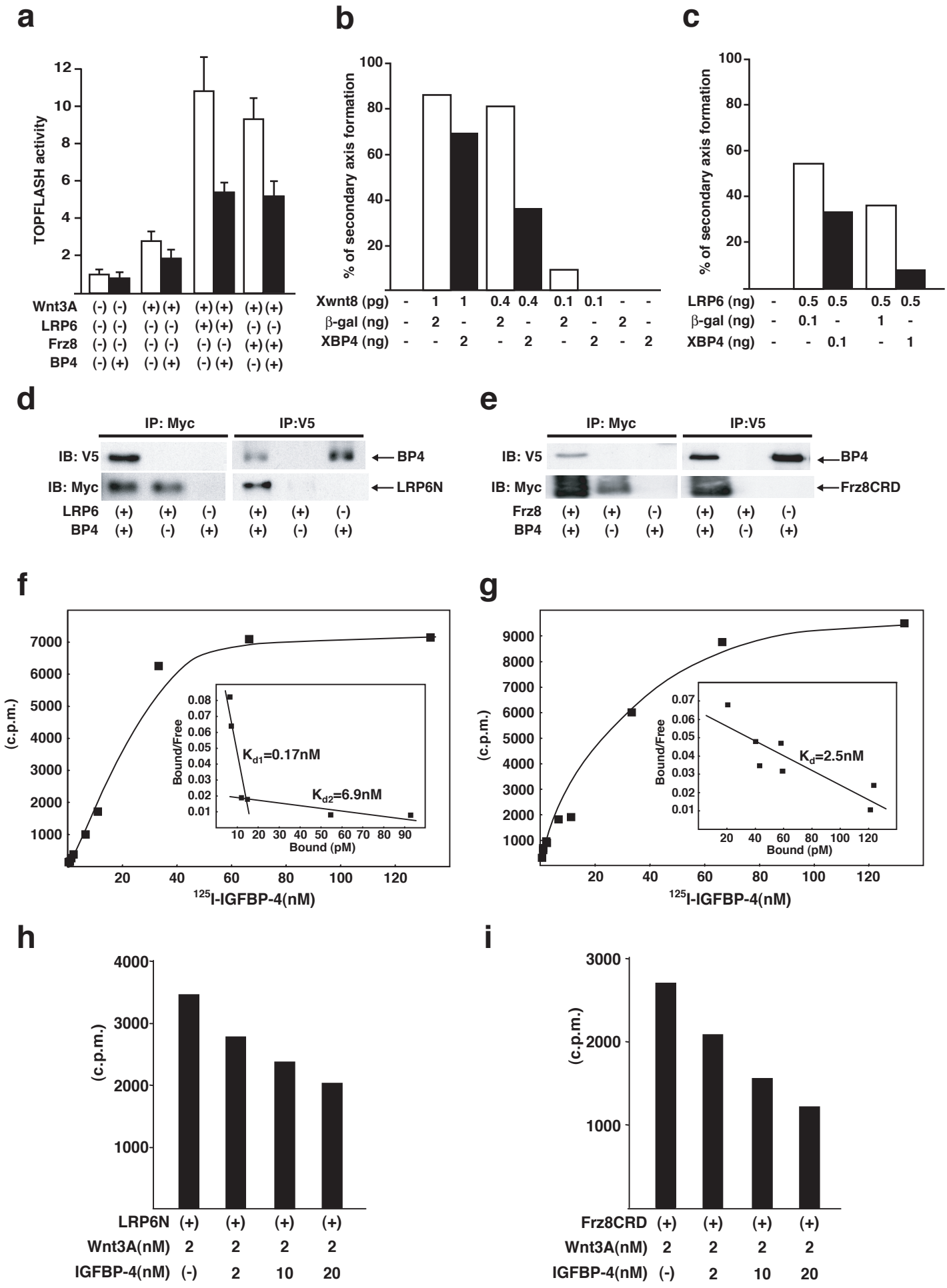
a
TOPFLASH activity
Wnt3A (-) (-) (+) (+) (+) (+) (+) (+)
LRP6 (-) (-) (-) (-) (+) (+) (-) (-)
Frz8 (-) (-) (-) (-) (-) (-) (+) (+)
BP4 (-) (+) (-) (+) (-) (+) (-) (+)
b
% of secondary axis formation
Xwnt8 (pg) - 1 1 0.4 0.4 0.1 0.1 - -
β-gal (ng) - 2 - 2 - 2 - 2 -
XBP4 (ng) - - 2 - 2 - 2 - 2
c
% of secondary axis formation
LRP6 (ng) - 0.5 0.5 0.5 0.5
β-gal (ng) - 0.1 - 1 -
XBP4 (ng) - - 0.1 - 1
d
IP: Myc
IP:V5
IB: V5
IB: Myc
BP4
LRP6N
LRP6 (+) (+) (-) (+) (+) (-)
BP4 (+) (-) (+) (+) (-) (+)
e
IP: Myc
IP:V5
IB: V5
IB: Myc
BP4
Frz8CRD
Frz8 (+) (+) (-) (+) (+) (-)
BP4 (+) (-) (+) (+) (-) (+)
f
(c.p.m.)
Bound/Free
Kd1=0.17nM
Kd2=6.9nM
Bound (pM)
125I-IGFBP-4(nM)
g
(c.p.m.)
Bound/Free
Kd=2.5nM
Bound (pM)
125I-IGFBP-4(nM)
h
(c.p.m.)
LRP6N (+) (+) (+) (+)
Wnt3A(nM) 2 2 2 2
IGFBP-4(nM) (-) 2 10 20
i
(c.p.m.)
Frz8CRD (+) (+) (+) (+)
Wnt3A(nM) 2 2 2 2
IGFBP-4(nM) (-) 2 10 20

Figure 3

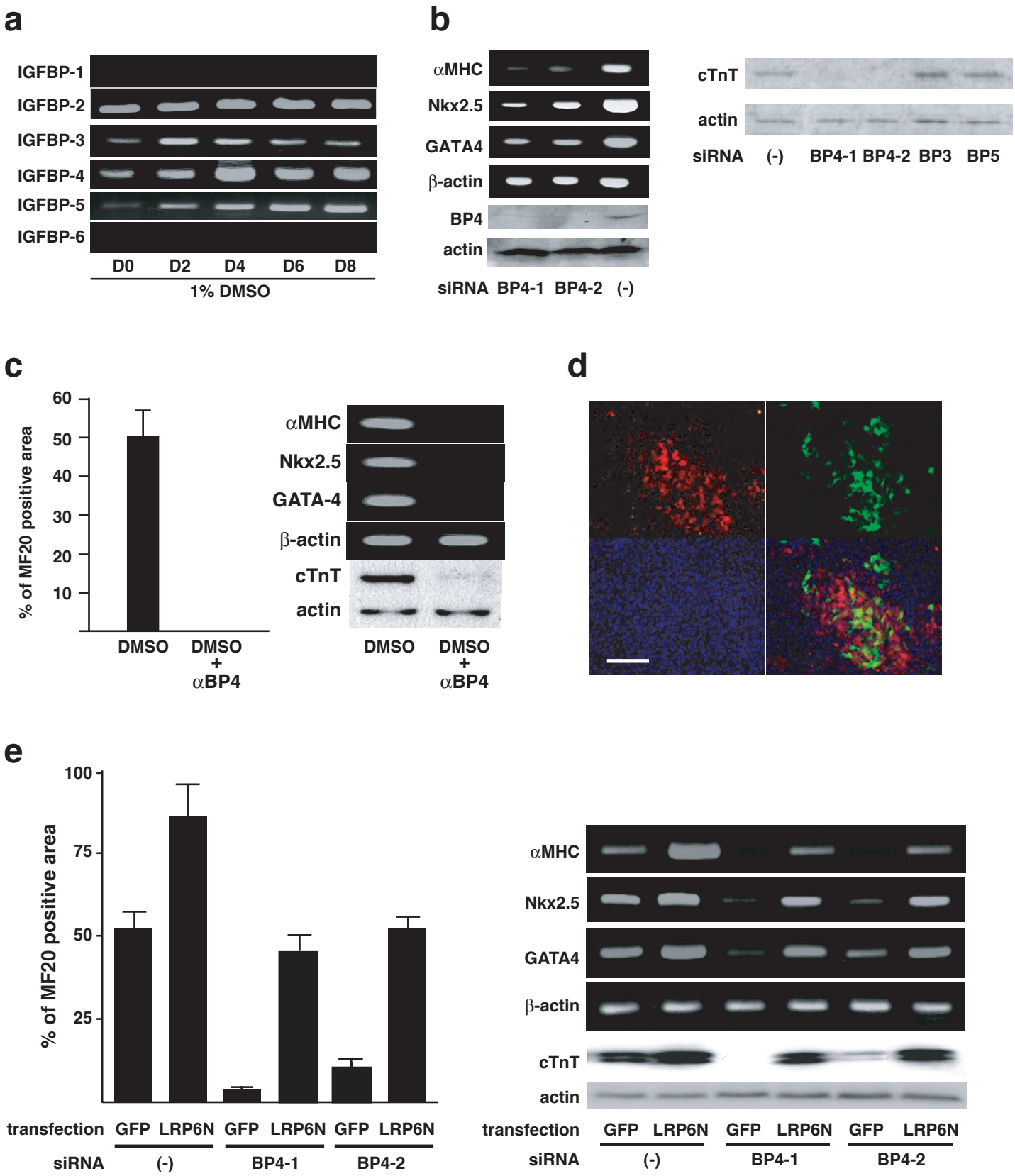
a
IGFBP-1
IGFBP-2
IGFBP-3
IGFBP-4
IGFBP-5
IGFBP-6
D0 D2 D4 D6 D8
1% DMSO
b
αMHC
Nkx2.5
GATA4
β-actin
BP4
actin
siRNA BP4-1 BP4-2 (-)
cTnT
actin
siRNA (-) BP4-1 BP4-2 BP3 BP5
c
% of MF20 positive area
60
50
40
30
20
10
DMSO
DMSO + αBP4
αMHC
Nkx2.5
GATA-4
β-actin
cTnT
actin
DMSO
DMSO + αBP4
d
e
% of MF20 positive area
100
75
50
25
transfection GFP LRP6N GFP LRP6N GFP LRP6N
siRNA (-) BP4-1 BP4-2
αMHC
Nkx2.5
GATA4
β-actin
cTnT
actin
transfection GFP LRP6N GFP LRP6N GFP LRP6N
siRNA (-) BP4-1 BP4-2

Figure 4

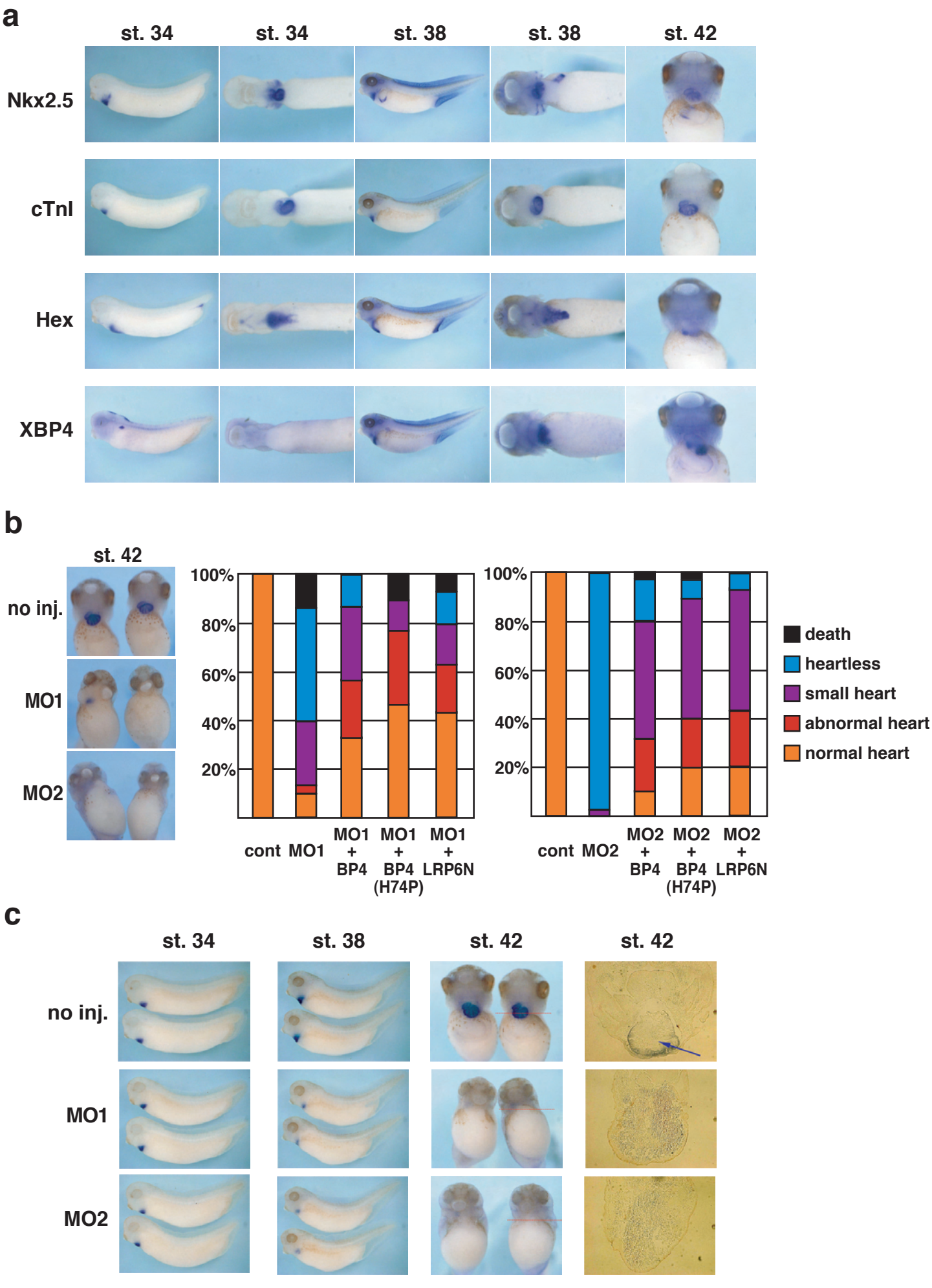
a
st. 34
st. 34
st. 38
st. 38
st. 42
Nkx2.5
cTnI
Hex
XBP4
b
st. 42
no inj.
MO1
MO2
100%
80%
60%
40%
20%
cont
MO1
MO1 + BP4
MO1 + BP4 (H74P)
MO1 + LRP6N
MO2
MO2 + BP4
MO2 + BP4 (H74P)
MO2 + LRP6N
death
heartless
small heart
abnormal heart
normal heart
c
st. 34
st. 38
st. 42
st. 42
no inj.
MO1
MO2

Supplementary Figure S1

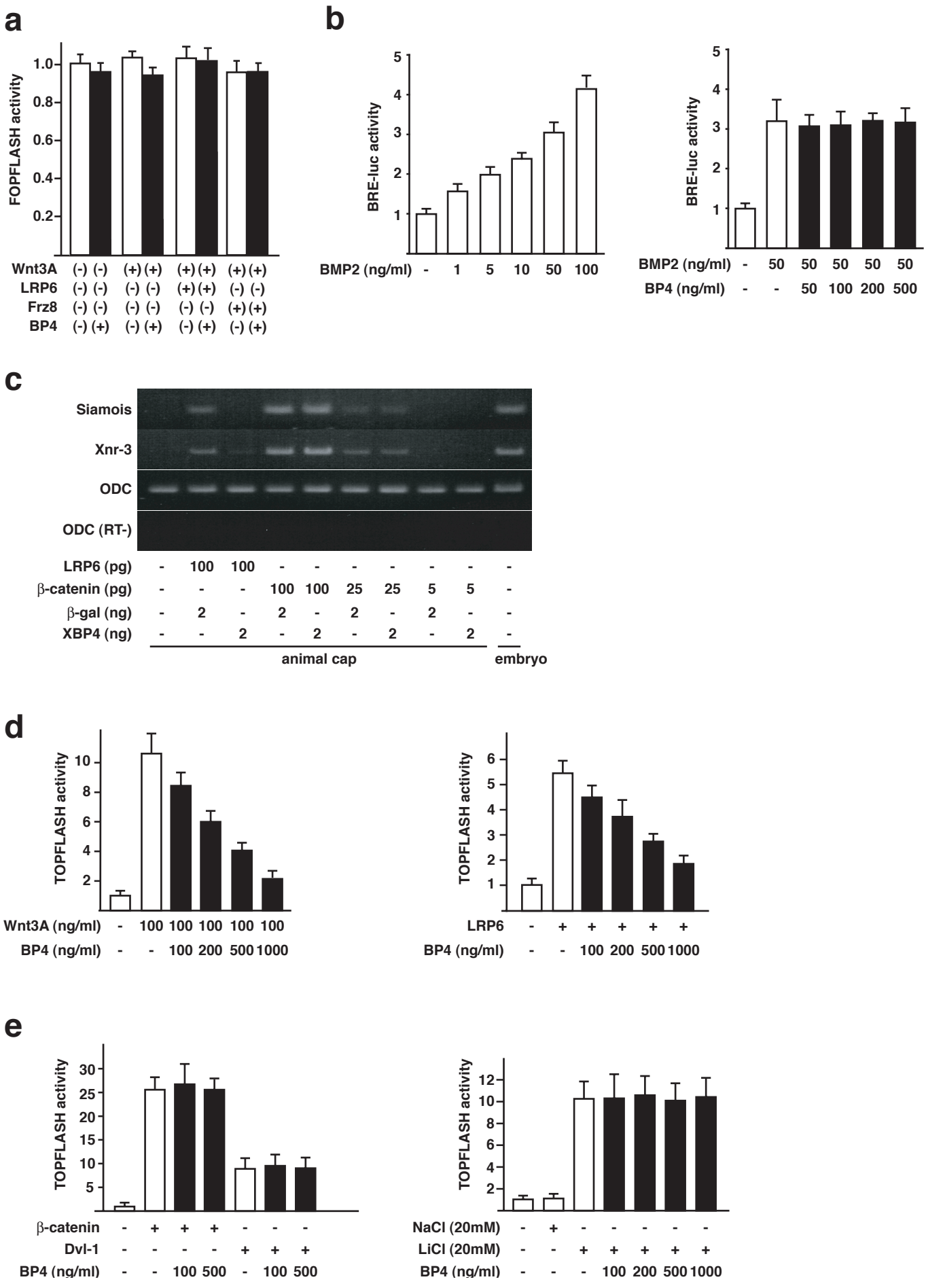

Supplementary Figure S2

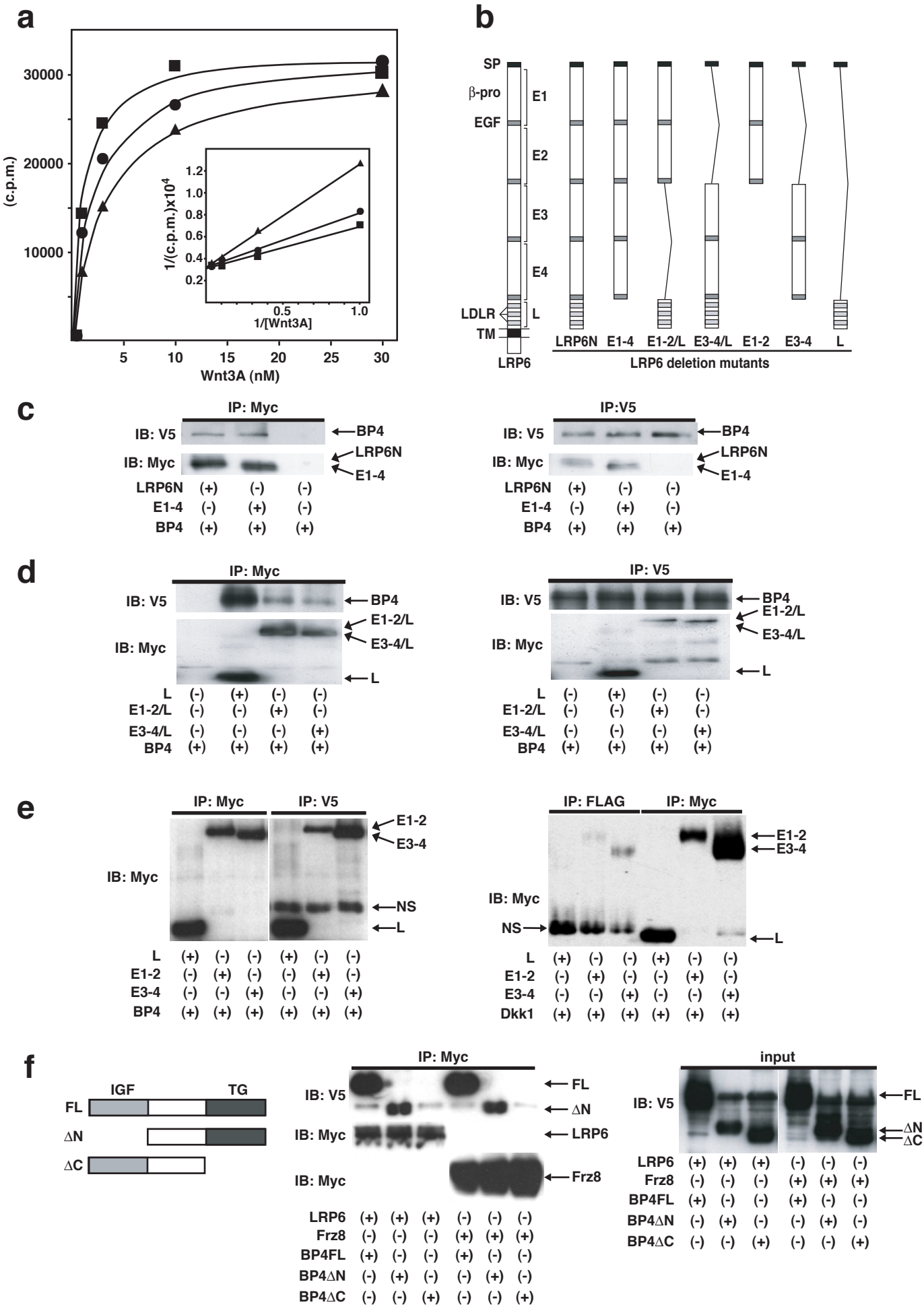

Supplementary Figure S3

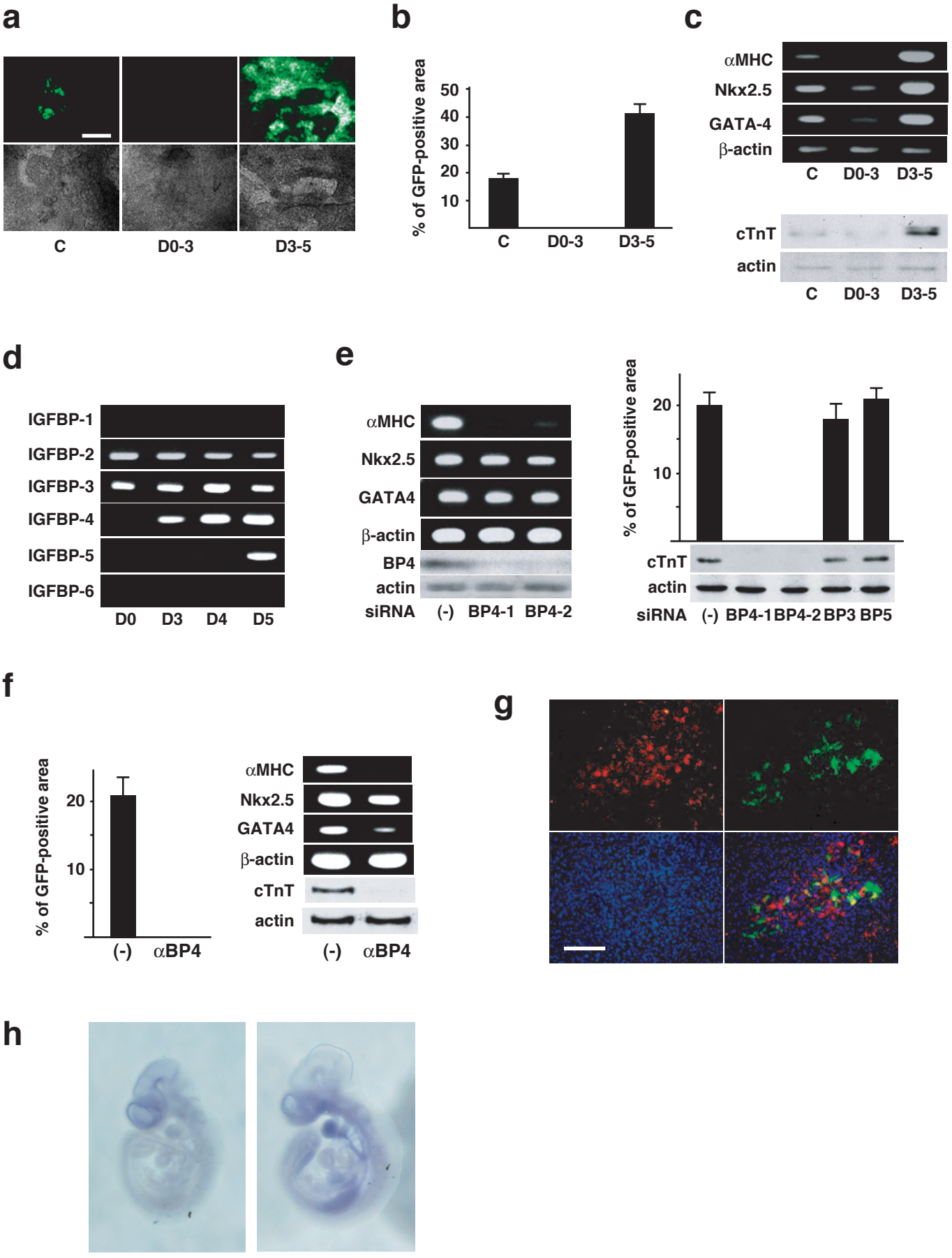

Supplementary Figure S4

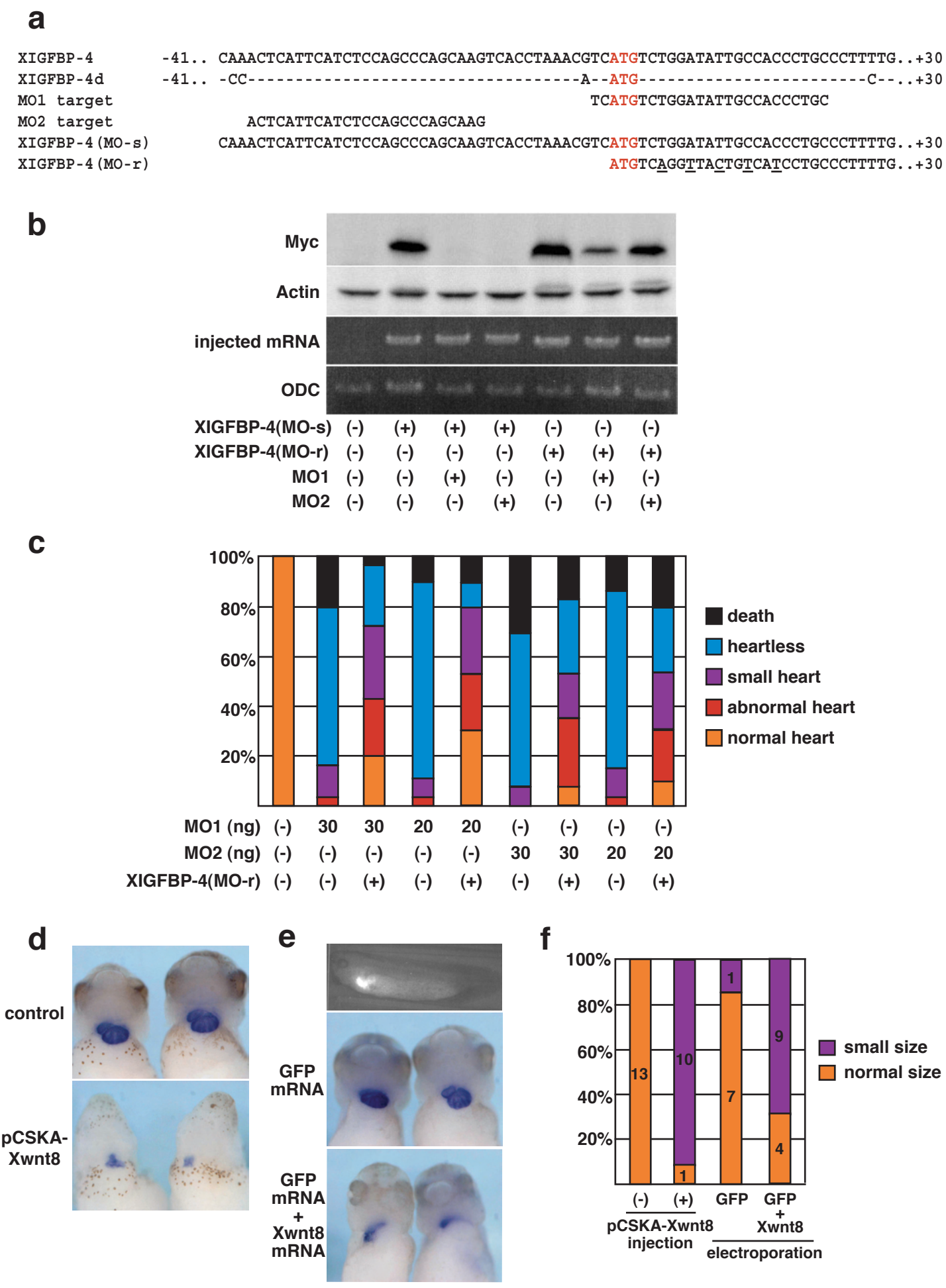

Supplementary Figure S5